Chaos, Solitons and Fractals 92 (2016) 115–122

Contents lists available at ScienceDirect

Chaos, Solitons and Fractals

Nonlinear Science, and Nonequilibrium and Complex Phenomena

journal homepage: www.elsevier.com/locate/chaos

Reaction front propagation of actin polymerization in a comb-reaction system

A. Iomin[a,*], V. Zaburdaev[b], T. Pfohl[c]

[a] Department of Physics, Technion, Haifa, 32000, Israel
[b] Max-Planck-Institute for the Physics of Complex Systems, Nüthnitzer Str. 38 Dresden, D-01187, Germany
[c] Department of Chemistry, University of Basel, Klingelbergstrasse 80 Basel CH-4056, Switzerland

ARTICLE INFO

Article history:
Received 27 January 2016
Revised 11 July 2016
Accepted 12 September 2016

Keywords:
Comb model
Subdiffusion
Actin polymerization
Reaction front
Hyperbolic scaling

ABSTRACT

We develop a theoretical model of anomalous transport with polymerization-reaction dynamics. We are motivated by the experimental problem of actin polymerization occurring in a microfluidic device with a comb-like geometry. Depending on the concentration of reagents, two limiting regimes for the propagation of reaction are recovered: the failure of the reaction front propagation and a finite speed of the reaction front corresponding to the Fisher-Kolmogorov-Petrovskii-Piscounov (FKPP) at the long time asymptotic regime. To predict the relevance of these regimes we obtain an explicit expression for the transient time as a function of geometry and parameters of the experimental setup. Explicit analytical expressions of the reaction front velocity are obtained as functions of the experimental setup.

1. Introduction

Microfluidics is an indispensable tool of modern bio-physical research. It allows to perform complex single-cell experiments with an immense throughput and high level of control. A flexible design allows for custom geometries and control of flows and chemical reactions. Recently, to probe the dynamics of actin polymerization, as well as to use the geometry of microfluidic device having the main supply channel with numerous identical side channels or chambers of different shapes, the following experimental setup, shown in Fig. 1, has been suggested [1,2]. The main channel serves to deliver and fill the side chambers with reagents where the corresponding reactions can be observed. The flow in the main channel and diffusion in the side-channels are dominating means of transport in such devices. Remarkably, the process of diffusion in this particular geometry was extensively studied in the context of anomalous diffusion. It is known as a comb model [3–5] and it was demonstrated that the transport of particles along the main channel (called backbone in the model) can become subdiffusive when the particles get trapped by diffusing into the side channels. Until recently it was mostly an abstract model, which was, however, extremely useful in understanding the principles of anomalous subdiffusive transport. In particular, the comb model was introduced for understanding the anomalous transport in percolating clusters [3,4] and it was considered as a toy model for a porous medium used for exploration of low dimensional percolation clusters [3,6]. It is a particular example of a non-Markovian phenomenon, which was explained within the framework of continuous time random walks [4,7,8]. Nowadays, comb-like models are widely used to describe different experimental applications like the transport in low-dimensional composites [9], the transport of calcium in spiny dendrites [10–12]. They also play an important role in developing the effective comb-shaped configuration of antennas [13] and modeling and simulating flows in the cardiovascular and ventilatory systems, related to techniques of virtual physiology [14].

The experimental setup on actin polymerization [1,15] is the direct implementation of the comb model, where the effects of complex diffusion should have a substantial effect on the observed phenomena. Interestingly, the comb structure not only leads to an anomaly in transport but also to a very remarkable effects on the propagation of chemical reactions [12].

The goal of this paper is to combine the consideration of anomalous transport and reaction dynamics to provide the theoretical grounds for the corresponding experimental efforts. Our analytical results on reaction propagation can help to guide the design of microfluidic devices but also can lead to real experimental tests of anomalous diffusion and reaction dynamics. For the reaction of polymerization, depending on the concentration of reagents we can recover such remarkable phenomena as the failure of the reaction front propagation [16,17] or a finite speed, which eventually leads to a Fisher-Kolmogorov-Petrovskii-Piscounov (FKPP) long

* Corresponding author. Fax: 972-4-829-5755.
E-mail addresses: iomin@physics.technion.ac.il (A. Iomin), vzaburd@pks.mpg.de (V. Zaburdaev), thomas.pfohl@unibas.ch (T. Pfohl).

http://dx.doi.org/10.1016/j.chaos.2016.09.011
0960-0779/

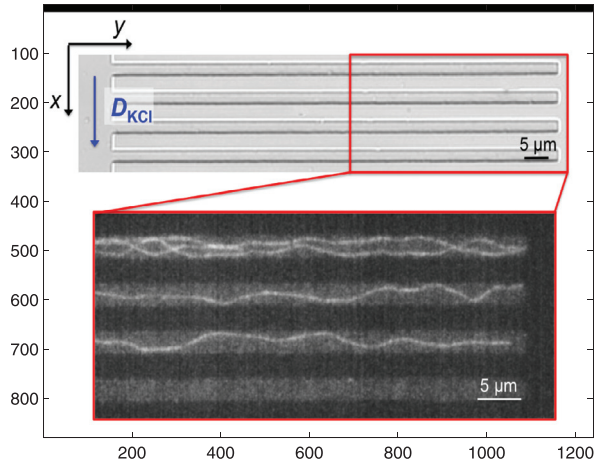

Fig. 1. (Color online) Optical micrograph of a segment of the microfluidics comb-like structures (on top). On bottom: microfluidic micrographs of fluorescently-labeled, polymerized actin filaments in a comb-like structure.

time asymptotic regime [18,19]. In the finite comb geometry of the experimental setup, these two processes correspond to different time scales. While the FKPP is a long time asymptotic regime, the reaction front propagation at subdiffusion is a transient process and takes place on the intermediate asymptotic times. A rigorous derivation of the governing equations allowed us to calculate the characteristic time scale separating these regimes explicitly. This time scale is determined by the geometry of the microfluidic device and be used to tune the regimes of diffusion and reactions in experiments.

1.1. Experimental setup

To study the dynamics of actin polymerization in diffusion controlled comb-like structures, we refer to a multi-height microfluidic device [1]. The microfluidic system consists of a main channel with a width $h_1 = 5$ μm, connected with comb-like structures that are smaller in width $h_2 = 0.5$ μm. Since the height of the main channel is ten-fold larger than that of the comb-like structures, a diffusion interface between the main, advective channel and the comb-like structure is generated due to the large hydraulic resistance of the connecting structures. Therefore, it is possible to add a solution of polymerization-inducing KCl to a solution of monomeric fluorescently labeled actin, including ATP necessary for in vitro polymerization, through the main channel, whereby KCl will diffuse into the comb-like structure and induce the polymerization of actin monomers into filaments. Similarly, magnesium (Mg^{2+}) can be used to induce the assembly of actin filaments into fibers. In what follows we will consider a very general reaction scheme referring to magnesium or KCl as an inducer, and the reaction itself as a reaction of polymerization. In experiments, the design of the side chambers can be varied and they can, for example, have circular or rectangular shapes. These shapes can also be incorporated into the analytical approach we develop below.

2. Mapping of the Laplace operator on a comb equation

Mapping the Laplace operators, acting in a three dimensional continuous-discrete geometry, as in Fig. 1, on a continuous two dimensional comb model equation, is related to averaging in the *xyz*-space [20–22] over some characteristic volume.

Anomalous diffusion of the inducer on the comb is described by the two dimensional probability distribution function (PDF) $P(x, y, t)$, and a special condition is that the displacement in the x direction is only possible along the structure axis (x-axis at $y = 0$). Therefore, this two dimensional diffusion is determined by the diagonal components of a diffusion tensor, where $D_x(y) = D_x\delta(y)$ and D_y are the diffusion coefficients in the x and y directions, correspondingly. In this case, the process of mapping of the Laplace operator on the comb model corresponds to establishing relations between the geometry parameters of geometrical constraint for the Laplace operator and the transport constants D_x and D_y.

In reality, we have the Laplace operator, which acts on the distribution function in a bulk of the main channel $P(x, y, z) = P_b(x, y, z)$ and in fingers (side channels, where reactions take place) $P(x, y, z) = P_f(x, y, z)$. Therefore, the following algorithm of mapping can be suggested. In the bulk of an infinite length along the x coordinate and yz surface with a cross-section $a \times a$, one has for the Laplace operator

$$D\Delta P_b(x, y, z) = D(\partial_x^2 + \partial_y^2 + \partial_z^2)P(x, y, z)$$

with the diffusivity of the inducer D and boundary conditions for $P(x, y, z) = P_b(x, y, z)$

$$\partial_z P|_{z=-a/2} = \partial_z P|_{z=a/2} = \partial_y P|_{y=-a/2} = \partial_y P|_{y=a/2} = 0.$$

Integration over z leads to the disappearance of the z component of the Laplace operator due to the boundary condition. For the PDF, one obtains

$$\int_{-a/2}^{a/2} P_b(x, y, z)dz \approx aP_b(x, y, 0),$$

where we used the middle point theorem. Integration over y in the bulk yields zero except those y regions where the bulk is connected with the fingers. Plunging the fingers inside the bulk, one arrives at the dynamics along the backbone which is at $y = 0$. Note, that the process of "plunging" mathematically corresponds to use of the middle point theorem. Therefore, we have for the bulk diffusion at arbitrary x

$$\frac{1}{a^3}\int_{-a/2}^{a/2} dxdydz\Delta P_b(x, y, z) \approx D\partial_x^2 P(x, y = 0, z = 0) = D\delta(y/a)\partial_x^2 P(x, y). \quad (2.1)$$

Here we disregarded the z coordinate in the distribution function $P(x, y, z = 0) \equiv P(x, y)$.

Now we consider fingers, which have length h and their xz cross-section is $b \times b$. It is worth noting that to work with the symmetrical PDF, we are mapping the Laplace operator on a two-sided symmetrical comb model that is practically, reflected in a choice of the symmetric boundary conditions at $y = \pm h$. The Laplace operator with diffusivity d inside the fingers reads

$$d\Delta P_f(x, y, z) = d(\partial_x^2 + \partial_y^2 + \partial_z^2)P(x, y, z).$$

Taking into account the boundary conditions, integration/averaging over x and z leads to zero, except ∂_y^2 in periodic (in x) regions of the fingers at arbitrary x and $y \in [-h, h]$. We have for a single finger

$$\frac{1}{b^3}\int_{-b/2}^{b/2} dxdydz\partial_y^2 P(x, y, z) \approx \partial_y^2 P(x, y, z = 0).$$

Therefore, we obtain the average Laplace operator for the fingers with the finger density ρ

$$\frac{d}{b^3}\int_{-b/2}^{b/2} dxdydzd\Delta P_f(x, y, z) \approx \rho d\partial_y^2 P(x, y, z = 0). \quad (2.2)$$

The finger density ρ is a number of fingers on the interval of length a along the x direction. Without restriction of the generality we take $\rho \sim a/b$. Since z component disappears from the averaged Laplace operator, we disregard z again in the distribution function $P(x, y, z = 0) \equiv P(x, y)$.

After combining both Eqs. (2.1) and (2.2), we obtain an effective equation for the inducer transport along the comb structure with parameters related to the experimental geometry a, b and diffusion constants D and d

$$\partial_t P = aD\delta(y)\partial_x^2 P + d_\rho \partial_y^2 P. \tag{2.3}$$

Here $d_\rho = d\rho = D_y$ is the re-scaled diffusion coefficient and $aD = D_x$, which both establish the relation with the diffusion tensor of the comb model [6]. It is worth noting that the diffusion coefficient in x direction is $D(y) = aD\delta(y) = D\delta(y/a)$. The scaling of the δ function by a is convenient and valid in the limit $h \to \infty$, as well.

One should recognize that the singularity of the diffusion coefficient results from the mapping of the Laplace operator on the comb equation (2.3); it is the intrinsic transport property of the comb model. Note that this singularity of the diffusion coefficient is not trivial and is related to a non-zero flux along the x coordinates [21,23]. Integrating Eq. (2.3) over y from $-\epsilon/2$ to $\epsilon/2$: $\int_{-\epsilon/2}^{\epsilon/2} dy \ldots$, one obtains for the l.h.s. of the equation, after application of the middle point theorem, $\epsilon\partial_t P(x, y = 0, t)$, which is exact in the limit $\epsilon \to 0$. This term can be neglected in the limit $\epsilon \to 0$. Considering the r.h.s. of the integration, we obtain that the term responsible for the transport in the y direction reads

$$d_\rho \partial_y \Big[P(x, y, t)\big|_{y=\epsilon/2} - P(x, y, t)\big|_{y=-\epsilon/2} \Big].$$

This corresponds to the two outgoing fluxes from the backbone in the $\pm$ y directions: $F_{+y} + F_{-y}$. The transport in the x direction, after integration, is

$$\epsilon D(y \to 0)\partial_x^2 P(x, y = 0, t) = F_{x;y=0} \equiv F_x.$$

Here, we take a general diffusivity function in the x direction $D(y)$ (instead of $aD\delta(y)$ in Eq. (2.3)). It should be stressed that the second derivative over x, presented in the form $\epsilon\partial_x^2 P = [\partial_x P(x + \epsilon/2) - \partial_x P(x - \epsilon/2)]$, ensures both incoming and outgoing fluxes for F_x along the x direction at a point x. Following the Kirchhoff's law, we have $F_x + F_{+y} + F_{-y} = 0$ for every point x and at $y = 0$. Function F_x contains both incoming and outgoing fluxes of the probability, while F_{+y} and F_{-y} are both outgoing probability fluxes. If the latter outgoing fluxes are not zero, the flux F_x has to be nonzero as well: $F_x \neq 0$, as containing an incoming flux. Therefore, $\epsilon D(y \to 0) \neq 0$. Taking $D(y) = \frac{\epsilon aD}{\pi(y^2+\epsilon^2)}$, one obtains in the limit $\epsilon \to 0$ a nonzero flux F_x with $D(y) = Da\delta(y)$, which is the diffusion coefficient in the x direction in Eq. (2.3). It is worth noting that this transport property of the comb model makes it possible to map the general Laplace operator of the experimental setup on the comb model by keeping "isomorphism" for the geometry, or the "topology" of the probability/contaminant fluxes.

Finally, the boundary conditions for Eq. (2.3) are $P(x = \pm\infty, y, t) = \partial_x P(x = \pm\infty, y, t) = 0$ and $\partial_y P(x, y = \pm h, t) = 0$, and the initial condition is $P(x, y, t = 0) = P_0(x)\delta(y)$. Such a localized initial condition and the absence of the convective flows can also be achieved experimentally.

3. Reaction-transport in a comb

Amending the comb Eq. (2.3) with a reaction term $\rho \cdot C(P)$, which also accounts for the density of fingers, we have

$$\partial_t P = D\delta(y/a)\partial_x^2 P + d_\rho \partial_y^2 P - \rho C(P). \tag{3.1}$$

The above Eq. (3.1) describes anomalous diffusion of an inducer in a comb structure together with the reaction of actin polymerization. In the simplest case, the reaction term $C(P)$ is described by the second order reaction equation (see Appendix A for details):

$$\frac{dP}{dt} = -k(N - P_0 + P)P, \tag{3.2}$$

where N is the initial concentration of actin, while k is the rate constant of the reaction.

3.1. Solution of linear reaction-transport comb equation: extinction dynamics

If during the reaction time $N - P_0 \gg P$ and $N \gg P_0$ (there is much more of actin than inducer), then the second order reaction Eq. (3.2) can be simplified to the first order

$$\frac{dP}{dt} = -kNP. \tag{3.3}$$

Substituting Eq. (3.3) into Eq. (3.1) yields

$$\partial_t P = Da\delta(y)\partial_x^2 P + d_\rho \partial_y^2 P - CP, \tag{3.4}$$

where $C = \rho \cdot k \cdot N$ is the constant reaction rate.

The reaction term disappears from Eq. (3.4) by the substitution

$$P = e^{-Ct}\tilde{P}.$$

The next step is the Laplace transform $\hat{\mathcal{L}}[\tilde{P}](t) = \tilde{P}(s)$, which turns Eq. (3.4) to

$$s\tilde{P} = Da\delta(y)\partial_x^2 \tilde{P} + d_\rho \partial_y^2 \tilde{P} + P_0\delta(y). \tag{3.5}$$

Its solution can be considered as a product $\tilde{P}(x, y, s) = \tilde{n}(y, s)f(x, s)$. The solution inside the fingers is found from the equation in the Laplace domain

$$s\tilde{n}(y) = d_\rho \partial_y^2 \tilde{n}(y)$$

with the boundary condition $\partial_y \tilde{n}(y)|_{y=\pm h} = 0$, which yields

$$\tilde{n}(y, s) = \frac{\cosh\left[(h - |y|)\sqrt{s/d_\rho}\right]}{\cosh\left[h\sqrt{s/d_\rho}\right]} \tag{3.6}$$

and $n(y = 0) = 1$.

As the solution is sought for in the form

$$\tilde{P}(x, y, s) = \tilde{n}(y, s)f(x, s), \tag{3.7}$$

we can write for its second derivative over y

$$\partial_y^2 \tilde{P} = \left\{ -2\delta(y)\sqrt{s/d_\rho}\frac{\sinh\left[(h - |y|)\sqrt{s/d_\rho}\right]}{\cosh\left[h\sqrt{s/d_\rho}\right]} + [s/d_\rho]\tilde{n}(y) \right\} f(x, s).$$

Therefore diffusion of the inducer in the bulk-backbone, determined by $f(x, s)$, is described by the following equation

$$Da\partial_x^2 f - 2\sqrt{sd_\rho}\tanh\left[h\sqrt{s/d_\rho}\right]f + P_0 = 0. \tag{3.8}$$

The presence of the hyperbolic tangent distinguishes two time scales and corresponding regimes. At a short time scale, when $h\sqrt{s/d_\rho} \gg 1$, we have

$$\tanh[h\sqrt{s/d_\rho}] \approx 1$$

and

$$D_{\frac{1}{2}}\partial_x^2 f - \sqrt{s}f + f_0 = 0, \tag{3.9}$$

where

$$D_{\frac{1}{2}} = \frac{Da}{2\sqrt{d_\rho}} = \frac{D\sqrt{ab}}{2\sqrt{d}} \tag{3.10}$$

is a generalized diffusion coefficient[1] and $f_0(x) = P_0(x) = P_0\delta(x)$, for simplicity. It should be admitted that the generalized diffusion coefficient in the x direction is independent of the finger's lengths h.

[1] Note that $\rho = a/b$.

By performing the Fourier transform $\tilde{f}(k)=\hat{\mathcal{F}}[f(x)]$, we obtain

$$\tilde{f}(k,s)=\frac{P_0}{\sqrt{s}+D_{\frac12}k^2}. \tag{3.11}$$

After the Laplace inversion of the solution (3.11) and taking into account a definition of the Mittag-Leffler function [24]

$$E_{\alpha,\beta}(z)=\frac{1}{2\pi i}\int_G\frac{r^{\alpha-\beta}e^r}{r^\alpha-z}dr,\quad \alpha,\beta>0,$$

we arrive at the solution

$$\tilde{f}(k,t)=\frac{P_0}{2\pi i}\int_{\sigma-i\infty}^{\sigma+i\infty}\frac{e^{st}ds}{\sqrt{s}+D_{\frac12}k^2}=\frac{P_0}{\sqrt{t}}E_{\frac12,\frac12}\left(-D_{\frac12}k^2t^{\frac12}\right). \tag{3.12}$$

Inverse Fourier transform of Eq. (3.12) yields a solution in terms of the Fox function [8]. However, this solution is valid for the "short" time-scale $t\ll\frac{h^2}{d_\rho}=\frac{h^2b}{da}$. Therefore, it is instructive to obtain an approximation of the solution in terms of analytical functions. Using the property $E_{a,b}(z)=zE_{a,a+b}(z)+1/\Gamma(b)$ for the two parameter Mittag-Leffler functions [25], and taking into account that the Mittag-Leffler function $E_{a,\,1}(z)$ of a small argument ($|z|\ll1$ and $z<0$) can be approximated by exponentials [8,24], we obtain

$$E_{\frac12,\frac12}\left(-D_{\frac12}k^2t^{\frac12}\right)\approx-D_{\frac12}k^2t^{\frac12}\exp\left[-\frac{D_{\frac12}k^2t^{\frac12}}{\Gamma(3/2)}\right]+\frac{1}{\Gamma(1/2)},$$

where $\Gamma(3/2)=(1/2)\Gamma(1/2)=\sqrt{\pi}/2$ is the gamma function. Now the Fourier inversion can be easily performed that yields for the approximation

$$\left[\frac{\Gamma(3/2)}{4\pi D_{\frac12}t^{\frac12}}\right]^{\frac12}\frac{d^2}{dx^2}\exp\left[-\frac{x^2\Gamma(3/2)}{4D_{\frac12}\sqrt{t}}\right].$$

Taking into account the reaction term, we obtain the short-time scale solution for extinct diffusion in the bulk

$$P(x,y=0,t<t_0)=\frac{P_0e^{-Ct}\delta(x)}{\sqrt{\pi t}}+\frac{P_0e^{-Ct}D_{\frac12}^{\frac12}}{2(4\pi t)^{\frac14}}\frac{d^2}{dx^2}\exp\left(-\frac{\sqrt{\pi}x^2}{8D_{\frac12}\sqrt{t}}\right). \tag{3.13}$$

Note, that this result is relevant for the time scale $t\ll\frac{h^2}{d_\rho}$ and is independent of h that corresponds to the limit of $h\to\infty$, as well.

On a long time-scale, the hyperbolic tangent in Eq. (3.8) has a small argument:

$$\tanh[h\sqrt{s/d_\rho}]\approx h\sqrt{s/d_\rho}.$$

This corresponds to an equation for normal diffusion

$$D(a/2h)\partial_x^2f-sf+P_0/h=0,\qquad D(a/2h)\equiv\bar{D} \tag{3.14}$$

with a well-known solution. Finally this gives the long-time scale solution in the bulk

$$P(x,y=0,t>t_0)=e^{-Ct}\int dx'P_0(x')\frac{1}{\sqrt{\pi h^2\bar{D}t}}\times\exp\left(-\frac{(x-x')^2}{4\bar{D}t}\right). \tag{3.15}$$

When $P_0(x)=\delta(x)$, the Green function coincides with the distribution.

In Eqs. (3.13) and (3.15), we have seen that there is a distinct time scale separating the transport regimes. The corresponding transient time parameter

$$t_0=\frac{h^2}{d_\rho}=\frac{h^2b}{ad} \tag{3.16}$$

is determined from the geometry of the experiment.[2] We should note that due to the exponential pre-factor e^{-Ct} and depending on the parameters, initial subdiffusive dynamics maybe the only experimentally detectable regime.

4. Reaction front propagation in a case of high concentration of inducer

In the case when the concentration of the inducer is high enough, the approximation Eq. (3.3) is not valid anymore, and one has to take into account the second order reaction, Eq. (3.2). Thus the reaction term reads

$$C(P)=CP+C_1P^2,\quad C=\rho\cdot k\cdot(N-P_0),\quad C_1=\rho\cdot k. \tag{4.1}$$

In this nonlinear case, the exact analytical treatment of Eq. (3.1) is impossible, and we apply an analytical approximation to find the overall velocity of the reaction-polymerization front propagation without resolving the exact shape of the front, namely without knowledge of the exact distribution function $P(x, y, t)$.

Since we are seeking for the front propagation in the x direction, the exact shape in the y direction is not important, and we consider the distribution as a function of the x coordinate alone $P_1(x, t)$. In other words, the details of dynamics inside the fingers is not important, and we take into account its overall contribution to diffusion in the x axis. To this end, the y coordinate is integrated out

$$P_1(x,t)=\int_{-h}^{h}P(x,y,t)dy. \tag{4.2}$$

Therefore, this integration in Eq. (3.1) with the reaction term given in Eq. (4.1) yields an equation in an unclosed form. First of all, we take into account that

$$\int_{-h}^{h}\partial_y^2P(x,y,t)dy=\partial_yP(x,y,t)\Big|_{y=-h}^{y=h}=0.$$

This leads to

$$\partial_tP_1(x,t)=aD\partial_x^2P(x,y=0,t)-CP_1-C_1\int_{-h}^{h}P^2(x,y,t)dy. \tag{4.3}$$

Here, we have two problematic terms. The first one is $P(x,y=0,t)$, which will be expressed via $P_1(x, t)$. To this end we use the relation (3.7), where we pay attention to $\tilde{P}(x,y=0,s)=f(x,s)$. Integrating Eq. (3.7) over y yields

$$\tilde{P}_1(x,s)=\tilde{P}(x,y=0,s)\int_{-h}^{h}\tilde{n}(y,s)dy=2\tilde{P}(x,y=0,s)\int_0^h\tilde{n}(y,s)dy.$$

Therefore we can write

$$\tilde{P}(x,y=0,s)=\sqrt{s/4d_\rho}\tanh^{-1}\left[h\sqrt{s/d_\rho}\right]\cdot\tilde{P}_1. \tag{4.4}$$

Performing the inverse Laplace transform, we obtain from Eq. (4.4)

$$\begin{aligned}P(x,y=0,t)&=\frac{1}{2\pi i}\int_{\sigma-i\infty}^{\sigma+i\infty}ds\\&\quad\times\int_0^\infty dt_1dt_2P_1(x,t_1)\mathcal{R}_1(t_2)\cdot e^{-st_1}\cdot e^{-st_2}\cdot e^{st}\\&=\int_0^\infty dt_1\int_0^\infty dt_2P_1(t_1)\mathcal{R}_1(t_2)\delta(t-t_1-t_2)\\&=\int_0^t dt'P_1(t-t')\mathcal{R}_1(t').\end{aligned} \tag{4.5}$$

[2] Note that if $\rho=1$, then $t_0=h^2/d$, which coincides with the transient time of the "classical" comb model [26].

Here we take into account the causality principle $P(t-t_1)=0$ for $t_1 > t$, and introduce the kernel $\mathcal{R}_1(t)$ through the Laplace inversion

$$\mathcal{R}_1(t) = \hat{\mathcal{L}}^{-1}\left[\sqrt{s/4d_\rho}\tanh^{-1}\left(h\sqrt{s/d_\rho}\right)\right]. \tag{4.6}$$

The second problematic term is the integration of the nonlinear reaction. We present it in a form convenient for further analytical treatment. After performing a chain of transformations, presented in detail in Appendix B, we obtain

$$N.L.R.T. = \int_0^\infty dt_1 dt_2 P_1(x,t-t_1)P_1(x,t-t_2) \times \frac{1}{(2\pi i)^2}\int_{\sigma-i\infty}^{\sigma+i\infty}\tilde{\mathcal{R}}(s_1,s_2)e^{s_1t_1}\,e^{s_2t_2}ds_1\,ds_2. \tag{4.7}$$

In what follows we will denote this term as N.L.R.T. Finally, an equation for $P_1(x,t)$ reads

$$\partial_t P_1 = aD\partial_x^2\int_0^t \mathcal{R}_1(t')P_1(t-t')dt' - CP_1 - C_1\int_{-\infty}^t \mathcal{R}(t',t'')P_1(t-t')P_1(t-t'')dt'dt'', \tag{4.8}$$

where two-time-point kernel $\mathcal{R}(t',t'')$ is defined in the Laplace space, Eq. (4.7).

5. Hyperbolic scaling for the overall velocity of the reaction front propagation

To evaluate the overall velocity of the asymptotic front, we follow the hyperbolic scaling consideration, developed in [27,28] and adopted in [12] for consideration of the reaction transport front propagation in comb structures. Let us introduce a small parameter, say ε, at the derivatives with respect to time and space [27,28]. To this end we re-scale $x \to x/\varepsilon$ and $t \to t/\varepsilon$, while for the PDF we have

$$P_1(x,t) \to P_1^\varepsilon(x,t) = P_1\left(\frac{x}{\varepsilon},\frac{t}{\varepsilon}\right).$$

Therefore, one looks for the asymptotic solution in the form of the Green's approximation

$$P_1^\varepsilon(x,t) = \exp\left[-\frac{G^\varepsilon(x,t)}{\varepsilon}\right]. \tag{5.1}$$

The main strategy of implication of this construction is the limit $\varepsilon \to 0$ that yields an asymptotic behavior at finite x and t, where we have

$$\exp\left[-\frac{G^\varepsilon(x,t)}{\varepsilon}\right] = 0,$$

except for the condition when

$$G^\varepsilon(x,t) = 0.$$

This equation determines the position of the reaction spreading front, and in this limit, $G(x,t) = \lim_{\varepsilon\to 0} G^\varepsilon(x,t)$ is accounted as the principal Hamiltonian function [27,28]. Therefore, the Hamiltonian approach can be applied to calculate the propagation front velocity. In this case, partial derivatives of $G(x,t)$ with respect to time and coordinate have the physical meaning of the Hamiltonian and the momentum:

$$\frac{\partial G(x,t)}{\partial t} = -H, \qquad \frac{\partial G(x,t)}{\partial x} = p. \tag{5.2}$$

Now, the ansatz (5.1) for the PDF inside the bulk is inserted in Eq. (4.8), where we also make the scaling change $x \to \frac{x}{\varepsilon}$ and $t \to \frac{t}{\varepsilon}$.

Let us start from the last term in Eq. (4.8), which is the reaction term. First of all we take into account the following change in the upper limit of integrations

$$\int_{-\infty}^t dt' \Rightarrow \lim_{\varepsilon\to 0}\int_{-\infty}^{\frac{t}{\varepsilon}} dt' = \int_{-\infty}^\infty dt'.$$

Then, we make the following expansion for $P_1^\varepsilon(x,\frac{t}{\varepsilon}-t') \equiv P_1^\varepsilon(t-\varepsilon t')$, which reads

$$P_1^\varepsilon(t-\varepsilon t') = \exp\left[-\frac{1}{\varepsilon}G^\varepsilon(t-\varepsilon t')\right] \approx \exp\left[-\frac{1}{\varepsilon}G^\varepsilon(t)+t'\partial_t G^\varepsilon(t)\right].$$

Therefore, the nonlinear reaction term reads

$$N.L.R.T. = \frac{1}{(2\pi i)^2}e^{-2\frac{G^\varepsilon}{\varepsilon}}\cdot\int_{-\infty}^\infty dt'dt'' \times\int_{\sigma-i\infty}^{\sigma+i\infty}\tilde{\mathcal{R}}(s',s'')e^{-(H-s')t'}\,e^{-(H-s'')t''}ds'ds'', \tag{5.3}$$

where we use the first equation in (5.2). Integration over s' and s'' is performed with some care, since $\tilde{\mathcal{R}}$ is singular at $s'=\pm s''$. The main result here is that $\tilde{\mathcal{R}}$ is finite and $N.L.R.T. \sim e^{-2\frac{G^\varepsilon}{\varepsilon}}$, that in the limit $\varepsilon \to 0$ is of the order of $o(e^{-\frac{G^\varepsilon}{\varepsilon}})$. Therefore it does not contribute to the final result, as the rest of the equation is of the order of $O(e^{-\frac{G^\varepsilon}{\varepsilon}})$.

Now we consider the kinetic term taking the time integration with $\mathcal{R}_1$ kernel. This reads

$$\int_0^{\frac{t}{\varepsilon}}\mathcal{R}_1(t')e^{-\frac{G^\varepsilon(t-\varepsilon t',x)}{\varepsilon}}dt' = e^{-\frac{G^\varepsilon(t)}{\varepsilon}}\int_0^\infty \mathcal{R}_1(t')e^{-Ht'}dt' = e^{-\frac{G^\varepsilon(t)}{\varepsilon}}\tilde{\mathcal{R}}_1(H),$$

where $\tilde{\mathcal{R}}_1(H)$ is defined in Eq. (4.6).

Finally, differentiating in the limit $\varepsilon \to 0$ where $(N.L.R.T. = 0)$ and taking into account that the Hamiltonian H and the momentum p in Eq. (5.2) are independent of x and t explicitly (which leads to the absence of mixed derivatives), one obtains that the kinetic Eq. (4.8) becomes a Hamilton-Jacobi equation:

$$-\partial_t G = aD(\partial_x G)^2\tilde{\mathcal{R}}_1(H) - C, \tag{5.4}$$

where $G \equiv G(x,t) = \lim_{\varepsilon\to 0} G^\varepsilon$ is the action (principal Hamiltonian function)

$$G(x,t) = \int_0^t [p(\tau)\dot{x}(\tau) - H(p(\tau),x(\tau))]d\tau.$$

The rate v at which the front moves is determined by the condition $G(x,t)=0$. Together with the Hamilton equations, this yields

$$v = \dot{x} = \frac{\partial H}{\partial p}, \quad v = \frac{H}{p}. \tag{5.5}$$

The first equation in (5.5) reflects the dispersion condition, while the second one is a result of the asymptotically free particle dynamics, when the action is $G(x,t) = px - Ht$. Eq. (5.5) is obtained by taking into account that $x = vt$. The combination of these two equations can be replaced[3] by

$$v = \min_{H>0}\frac{H}{p(H)} = \min_{p>0}\frac{H(p)}{p}. \tag{5.6}$$

To proceed, we take into account that $\partial_t G = -H$ and $\partial_x G = p$. We substitute these values in Eq. (5.4) and taking into account Eq. (4.6) for the kernel $\tilde{\mathcal{R}}_1(H)$, we obtain Eq. (5.4) in the form

$$H = D_{\frac{1}{2}}p^2\sqrt{H}\left[\tanh\left(\sqrt{Ht_0}\right)\right]^{-1} - C. \tag{5.7}$$

[3] Eq. (5.5) follows from the derivation $\partial_p(H/p) = (\partial_p H)/p - H/p^2 = 0$.

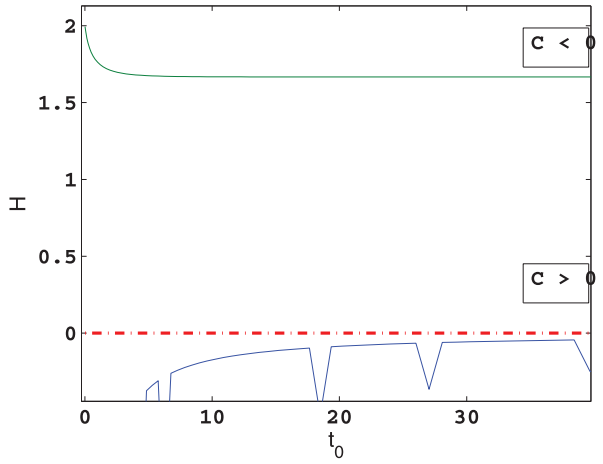

Fig. 2. (Color online) Numerical solutions of Eq. (5.8) for the Hamiltonian H vs. transient time t_0 for $C=-1$ (upper plot) and $C=1$ (lower plot). The transient time t_0 plays a role of a scaling parameter, which reflects various realizations of the comb geometry of the experimental setup, shown in Fig. 1.

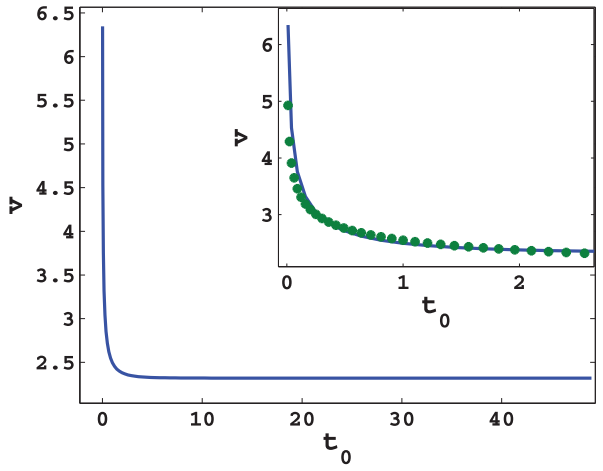

Fig. 3. (Color online) The overall velocity of the reaction front propagation v for different realizations of the experimental setup t_0 for $C=-1$ and $D_{\frac{1}{2}}=1$. The insert describes the result for the small values of t_0 (solid line). The fitting plot (*) corresponds to $t_0^{-1/4}$ curve.

The minimum condition Eq. (5.6) for this equation yields

$$(3H+5C)\cdot\sinh\left(2\sqrt{H\,t_0}\right)=2(H+C)\sqrt{H\,t_0}. \tag{5.8}$$

Numerical solutions of Eq. (5.8) for H vs. t_0 are presented in Fig. 2. These solutions determine the overall velocity of the reaction front propagation v for different realizations of the experimental setup, reflected by parameter $t_0=h^2b/ad$. The result of numerical calculations of the reaction front velocity is depicted in Fig. 3, where t_0 is the scaling parameter. It determines the dependence of the reaction front velocity v on the geometry of the experimental setups.

As obtained, the solutions depend on the reaction rate C. For $C>0$, there is no positive solutions for H, and the solution of Eq. (5.6) is at $H=0$ for all values of the scaling parameter t_0. For $C<0$, one obtains non-trivial solutions of Eqs. (5.6) and (5.8). We define two regimes with $t_0<1$ and $t_0>1$. The first one is the subdiffusive regime, when v is a constant function of t_0. In the second, diffusive regime, the front velocity is a decreasing function of t_0, as it is shown in the insert of Fig. 3. The fitting curve (marked by stars) in the insert is $v(t_0)\sim 1/t_0^{1/4}$.

Analytical solutions of Eqs. (5.6) and (5.8) can be also obtained in the limiting cases of t_0. As follows from the numerical solutions in Fig. 2, the physical values of the energy H are restricted inside the interval of the order of $H\sim 1$. In this case, the asymptotic solutions of Eqs. (5.6) and (5.8) are determined by the limiting values of the scaling parameter t_0. For the analytical estimation, we consider two regimes with $t_0\gg 1$ and $t_0\ll 1$. The first one is the subdiffusive regime, when v is independent of t_0. In the second, diffusive regime, the front velocity is a decreasing function of t_0, as it is shown in the insert of Fig. 3. In what follows we obtain analytical expressions for the velocities and scaling $v=v(t_0)$.

5.1. Subdiffusive regime $t_0\gg 1$

In the subdiffusive regime, we obtain

$$\tanh\left(\sqrt{Ht_0}\right)\approx 1 \quad\text{and}\quad 2(H+C)\sqrt{H\,t_0}/\sinh\left(2\sqrt{H\,t_0}\right)\approx 0,$$

which simplifies Eq. (5.8)

$$(3H+5C)=0. \tag{5.9}$$

This equation has no solution for $C>0$. Therefore, for $C>0$ and $H\geq 0$, the only solution for the front velocity is

$$v=\frac{H}{p(H)}=0.$$

This means the failure of the front propagation, as expected for the initial concentration of the inducer less than actin and is in complete agreement with numerics. For $C<0$ (that corresponds to $P_0>N$) there is a solution $H=5|C|/3$ that yields a nonzero velocity of the reaction front propagation at subdiffusion

$$v=\frac{H^{5/4}\sqrt{D_{\frac{1}{2}}}}{\sqrt{H+C}}=\left(\frac{5}{3}\right)^{\frac{5}{4}}\cdot\left(\frac{3}{2}\right)^{\frac{1}{2}}\cdot\left(D_{\frac{1}{2}}^2|C|^3\right)^{\frac{1}{4}}$$
$$=\left(\frac{5}{3}\right)^{\frac{5}{4}}\cdot\left(\frac{3}{2}\right)^{\frac{1}{2}}\cdot\left(\frac{D^2ab|C|^3}{2d}\right)^{\frac{1}{4}}. \tag{5.10}$$

As expected, this result depends on diffusivity of reagents and the geometry parameters a, and b . However, it is independent of the finger's length that makes it possible to arrive at the correct comb limit $h\to\infty$, when only subdiffusion takes place.

5.2. Diffusive regime $t_0\ll 1$

In the opposite case of the diffusion regime, when $t_0\ll 1$, we have

$$\tanh\left(\sqrt{H/d_\rho}\right)\approx\sinh\left(\sqrt{H/d_\rho}\right)\approx h\sqrt{H/d_\rho}.$$

Then for $C<0$ ($P_0>N$), we obtain from Eq. (5.8) that $H=2|C|$, and substituting this result in $v=H/p(H)$, we obtain

$$v=2\sqrt{|C|D_{\frac{1}{2}}}\cdot t_0^{-\frac{1}{4}} \tag{5.11}$$

For $C>0$, there is no solution of Eq. (5.8), and the result for the front velocity is $v=0$.

The same results can be obtained from Eq. (5.4), which in this limit reads

$$H=\bar{D}p^2-C, \tag{5.12}$$

where $\bar{D}$ is defined in Eq. (3.14) and $p=\sqrt{(H+C)/\bar{D}}$. This immediately yields

$$v=\min_{H>0}\left[\frac{H\bar{D}^{\frac{1}{2}}}{\sqrt{(H+C)}}\right]=0$$

for $H=0$, as expected for $C>0$.

The situation changes dramatically for $C<0$. In this case, the equation

$$\frac{\partial H}{\partial p}=\frac{H}{p}$$

yields

$$2\bar{D}p = \bar{D}p + \frac{|C|}{p},$$

and the solution is $p = \sqrt{|C|/\bar{D}}$. Finally, after substitution in the velocity equation we get

$$v = \min_{p>0} \frac{H(p)}{p} = \frac{\bar{D}p^2 + |C|}{p} = 2\sqrt{\bar{D}|C|}. \tag{5.13}$$

This is a well known FKPP result for the reaction front velocity with the scaled diffusivity $\bar{D}$. Taking into account that $D_{\frac{1}{2}} = \bar{D}\sqrt{t_0}$, one arrives at Eq. (5.11). As we obtained, in this regime the front velocity scales as $v \sim t_0^{-1/4} = (da/h^2 b)^{1/4}$. This analytical result corresponds to the numerical one, where the both results are depicted in the insert of Fig. 3.

5.3. Discussion

One should recognise that the evaluation of the overall velocity reaction front propagation in the framework of the hyperbolic scaling is in the complete agreement with the exact solution of the extinction dynamics. Indeed, as follows from solutions (3.13) and (3.15) for $C > 0$ (when the actin concentration is large than inducer), the velocity of the reaction front is zero. These results coincide completely with the numerical and analytical results obtained by the hyperbolic scaling in the framework of the Hamilton-Jacobi equation, when $v = 0$. For $C < 0$ the nonlinear term becomes important, however, as follows from solution (3.15), the velocity of the reaction front, obtained from the condition $|C|t - x^2/4\bar{D}t = 0$, yields the result of Eq. (5.13) $v = 2\sqrt{\bar{D}|C|}$. Therefore, for the FKPP dynamics, the linearization of the nonlinear reaction-transport equation leads to a good approximation for the velocity of the reaction front propagation. For the subdiffusive dynamics, the situation is more sophisticated for $C < 0$, since the linearization approach is not valid. In this case, the hyperbolic scaling in the framework of the Hamilton-Jacobi equation is the reliable approach to the problem.

6. Conclusion

In this paper we considered anomalous transport and reaction dynamics by providing the theoretical grounds for the possible experimental realization of actin polymerization in comb-like geometry. Different regimes for the reaction of polymerization have been considered, and depending on the concentration of reagents (magnesium, KCl and actin), we recovered both the failure of reaction front propagation and a finite speed corresponding to the FKPP long time asymptotic regime. Moreover, we demonstrated that the geometry of the device determines the time scale separating the transient regime of subdiffusive transport from normal diffusion. These analytical and numerical results on reaction propagation can help to guide the design of microfluidic devices which will make advantage of the calculated transport regimes. Furthermore, they suggest the experimental realization of anomalous diffusion and reaction dynamics in a flexible, controllable, and affordable way. An interplay between the geometry design and the reaction polymerization rate can leads to different realizations of the reaction-transport regimes. In particular, for the fast reaction, or low concentration of the inducer, polymerization can be terminated before the transition time t_0. This leads to the reaction subdiffusion process. In the opposite case of the high initial concentration of the inducer, one can observe a transition process from reaction subdiffusion to reaction diffusion. In the future it would be interesting to generalize our approach and include the flow in the back-bone channel to explore additional regimes in the operation of the microfluidic setup.

Acknowledgements

We would like to thank Zoe Swank for providing the experimental micrographs. A.I. gratefully acknowledges the hospitality of the Max-Planck-Institute for the Physics of Complex Systems and financial support from the Israel Science Foundation (ISF-1028).

Appendix A. Few points on reaction for definition of the reaction term

The reaction term $C(P)$ can be found from the following arguments, see e.g. [29]. For the reaction-polymerization, we use the following *stoichiometry* expression $A + B \Rightarrow C$, where

$[A]$ is concentration of actin

$[B]$ is concentration of inducer

$[C]$ is concentration of polymer

Here an inducer is both magnesium and KCl. In general case, we consider the second order reaction, and also take into account that $[B] = P(x, y, t)$. Therefore, we have

$$\frac{dP}{dt} = -kP \cdot [A]$$

with the reaction rate k and initial condition $[B(t=0)] \equiv P(t=0) = P_0$, $[A(t=0)] = [A]_0 = N$, $[C]_0 = 0$.

Let us express $[A]$ by P. We have

$$P \equiv [B] = [B]_0 - [C] = P_0 - [C],$$
$$[A] = [A]_0 - [C] = [A]_0 - P_0 + P.$$

Therefore the reaction equation reads

$$\frac{dP}{dt} = -k(N - P_0 + P)P. \tag{A.1}$$

If during the reaction time, $N - P_0 \gg P$ and $N \gg P_0$, the second order reaction Eq. (3.2) becomes of the first order

$$\frac{dP}{dt} = -kNP. \tag{A.2}$$

Substituting Eq. (A.2) in Eq. (3.1) and denoting $C = \rho \cdot k \cdot N$ yields Eq. (3.4).

Appendix B. Chain of transformation for N.L.R.T.

We have the following chain of transformations for the nonlinear reaction term

$$N.L.R.T. \equiv \int_{-h}^{h} P^2(x, y, t)dy.$$

Defining the PDF $P(x, y, t)$ by the Laplace invesrsion, in time we have

$$\begin{aligned}(2\pi i)^2 \cdot N.L.R.T. &= \int_{\sigma-i\infty}^{\sigma+i\infty} e^{s_1 t} ds_1 e^{s_2 t} ds_2 \\ &\times \int_{-h}^{h} \tilde{P}(x, y, s_1)\tilde{P}(x, y, s_2)dy \\ &= \int_{\sigma-i\infty}^{\sigma+i\infty} e^{s_1 t} ds_1 e^{s_2 t} ds_2 \tilde{P}(x, y=0, s_1)\tilde{P}(x, y=0, s_2) \\ &\times \int_{-h}^{h} \tilde{n}(y, s_1)\tilde{n}(s_2, y)dy.\end{aligned}$$

Taking into account the solution in Eq. (4.4), we have

$$(2\pi i)^2 \cdot N.L.R.T. =$$
$$= \int_{\sigma-i\infty}^{\sigma+i\infty} ds_1\, ds_2 \tilde{\mathcal{R}}(s_1, s_2)\tilde{P}_1(x, s_1)\tilde{P}_1(x, s_2)\frac{\sqrt{s_1 s_2}}{4d_\rho}$$

$$\times \tanh^{-1}\left[h\sqrt{s_1/d_\rho}\right]\cdot\tanh^{-1}\left[h\sqrt{s_2/d_\rho}\right]e^{s_1 t}\,e^{s_2 t}$$
$$= \int_0^\infty d\tau_1 d\tau_2 P_1(x,\tau_1)P_1(x,\tau_2)\int_{\sigma-i\infty}^{\sigma+i\infty} ds_1\,ds_2$$
$$\times \frac{\sqrt{s_1 s_2}}{4d_\rho}\cdot\tanh^{-1}\left[h\sqrt{s_1/d_\rho}\right]\cdot\tanh^{-1}\left[h\sqrt{s_2/d_\rho}\right]$$
$$\times e^{s_1(t-\tau_1)}\,e^{s_2(t-\tau_2)}\tilde{\mathcal{R}}(s_1,s_2),$$

where

$$\mathcal{R}(s_1,s_2)=\int_{-h}^{h}\tilde{n}(y,s_1)\tilde{n}(s_2,y)dy.$$

Introducing new variables $t-\tau_1=t_1$ and $t-\tau_2=t_2$, one obtains for the time integration

$$\int_0^\infty d\tau_1 = -\int_t^{-\infty} dt_1 = \int_{-\infty}^{t} dt_1,$$

and the same procedure is performed for τ_2. This finally, yields the N.L.R.T. in Eq. (4.7).

References

[1] Deshpande S, Pfohl T. Hierarchical self-assembly of actin in micro-confinements using microfluidics. Biomicrofluidics 2012;6:034120.
[2] Deshpande S, Pfohl T. Real-time dynamics of emerging actin networks in cell-mimicking compartments. PLoS ONE 2015;10:e0116521.
[3] White SR, Barma M. Field-induced drift and trapping in percolation networks. J Phys A 1984;17:2995.
[4] Weiss GH, Havlin S. Some properties of a random walk on a comb structure. Physica A 1986;134:474.
[5] Matan O, Havlin S, Staufler D. Scaling properties of diffusion on comb-like structures. J Phys A 1989;22:2867.
[6] Arkhincheev VE, Baskin EM. Anomalous diffusion and drift in a combmodel of percolation clasters. Sov Phys JETP 1991;73:161.
[7] Montroll EW, Shlesinger MF. The wonderful world of random walks. In: Lebowitz J, Montroll EW, editors. Studies in statistical mechanics, v. 11. Amsterdam: Noth–Holland; 1984.
[8] Metzler R, Klafter J. The random walk's guide to anomalous diffusion: a fractional dynamics approach. Phys Rep 2000;339:1.
[9] Shamiryan D, Baklanov MR, Lyons P, Beckx S, Boullart W, Maex K. Diffusion of solvents in thin porous films. Colloids Surf A 2007;300:111.
[10] Santamaria F, Wils S, De Shutter E, Augustine GJ. Anomalous diffusion in Purkinje cell dendrites caused by spines. Neuron 2006;52:635; Santamaria F, Wils S, De Shutter E, Augustine GJ. The diffusional properties of dendrites depend on the density of dendritic spines. Eur J Neurosci 2011;34:561.
[11] Fedotov S, Méndez V. Non-Markovian model for transport and reactions of particles in spiny dendrites. Phys Rev Lett 2008;101:218102.
[12] Iomin A, Méndez V. Reaction-subdiffusion front propagation in a comblike model of spiny dendrites. Phys Rev E 2013;88:012706.
[13] Chu LCY, Guha D, Antar YMM. Comb-shaped circularly polarised dielectric resonator antenna. IEEE Electron Lett 2006;42:785.
[14] Thiriet M. Tissue functioning and remodeling in the circulatory and ventilatory systems. New York: Springer; 2013.
[15] Köster S, Kierfeld J, Pfohl T. Characterization of single semiflexible filaments under geometric constraints. Eur Phys J E 2008;25:439.
[16] Froemberg D, Schmidt-Martens H, Sokolov IM, Sagués F. Front propagation in $a+b\to 2a$ reaction under subdiffusion. Phys Rev E 2008;78:011128; Froemberg D, Schmidt-Martens H, Sokolov IM, Sagués F. Asymptotic front behavior in an $a+b\to 2a$ reaction under subdiffusion. 2011;83:031101.
[17] Iomin A, Sokolov IM. Application of hyperbolic scaling for calculation of reaction-subdiffusion front propagation. Phys Rev E 2012;86:022101.
[18] Kolmogoroff A, Petrovskii I, Piscounoff N. étude de l'équation de la diffusion avec croissance de la quantité de matiére et son application à un probéme biologique. Mosc Univ Math Bull 1937;1:25.
[19] Fisher RA. The wave of advance of advantageous genes. Ann Eugenics 1937;7:355.
[20] Dykhne AM, Kondratenko PS, Matveev LV. Impurity transport in percolation media. JETP Lett 2004;80:410.
[21] Dvoretskaya OA, Kondratenko PS. Anomalous transport regimes and asymptotic concentration distributions in the presence of advection and diffusion on a comb structure. Phys Rev E 2009;79:041128.
[22] Dvoretskaya OA, Kondratenko PS, Matveev LV. Anomalous diffusion in generelized Dykhne model. JETP 2010;110:58.
[23] Lubashevskii IA, Zemlyanov AA. Continuum description of anomalous diffusion on a comb structure. J Exper Theor Phys 1998;87:700.
[24] Bateman H, Erdèlyi A. Higher transcendental functions. NY: McGraw-Hill; 1955.
[25] Haubold HJ, Mathai AM, Saxena RK. Mittag-Leffler functions and their applications. J Appl Math 2011;2011:298628.
[26] Bouchaud J-P, Georges A. Anomalous diffusion in disordered media: statistical mechanisms, models and physical applications. Phys Rep 1990;195:127.
[27] Freidlin M. Markov processes and differential equations: asymptotic problems.. Basel: Birkhauser; 1996.
[28] Fedotov S. Front propagation into an unstable state of reaction-transport systems. Phys Rev Lett 2001;86:926.
[29] Fogler HS. Elements of chemical reaction engineering. Upper Saddle River, N.J.: Pearson Educational International; 2006.